Cell, Vol. 93, 467–476, May 1, 1998, Copyright ©1998 by Cell Press

Nibrin, a Novel DNA Double-Strand Break Repair Protein, Is Mutated in Nijmegen Breakage Syndrome

Raymonda Varon,[1] Christine Vissinga,[2,14] Matthias Platzer,[3] Karen M. Cerosaletti,[2,14] Krystyna H. Chrzanowska,[4] Kathrin Saar,[5] Georg Beckmann,[6] Eva Seemanová,[7] Paul R. Cooper,[8] Norma J. Nowak,[8] Markus Stumm,[9] Corry M. R. Weemaes,[10] Richard A. Gatti,[11] Richard K. Wilson,[12] Martin Digweed,[1] André Rosenthal,[3] Karl Sperling,[1] Patrick Concannon,[2] and André Reis,[1,5,13]

[1]Institute of Human Genetics, Charité
Humboldt University
Augustenburger Platz 1
D-13353 Berlin, Germany
[2]Virginia Mason Research Center
and Department of Immunology
University of Washington School of Medicine
Seattle, Washington 98101
[3]Institute for Molecular Biology
Department of Genome Analysis
07745 Jena, Germany
[4]Department of Medical Genetics
Children's Memorial Health Institute
04-736 Warsaw, Poland
[5]Mikrosatellitenzentrum
Max-Delbrück Center
14059 Berlin, Germany
[6]Department of Bioinformatics
Max-Delbrück Center
13125 Berlin, Germany
[7]Department of Medical Genetics
Charles University
15018 Prague, Czech Republic
[8]Department of Human Genetics
Roswell Park Cancer Institute
Buffalo, New York 14263-0001
[9]Institute of Human Genetics
University of Magdeburg
39112 Magdeburg, Germany
[10]University Hospital of Nijmegen
6500 HB Nijmegen, The Netherlands
[11]Department of Pathology
UCLA School of Medicine
Los Angeles, California 90095-1732
[12]Washington University School of Medicine
Genome Sequencing Center
St. Louis, Missouri 63108

Summary

Nijmegen breakage syndrome (NBS) is an autosomal recessive chromosomal instability syndrome characterized by microcephaly, growth retardation, immunodeficiency, and cancer predisposition. Cells from NBS patients are hypersensitive to ionizing radiation with cytogenetic features indistinguishable from ataxia telangiectasia. We describe the positional cloning of a gene encoding a novel protein, nibrin. It contains two modules found in cell cycle checkpoint proteins, a forkhead-associated domain adjacent to a breast cancer carboxy-terminal domain. A truncating 5 bp deletion was identified in the majority of NBS patients, carrying a conserved marker haplotype. Five further truncating mutations were identified in patients with other distinct haplotypes. The domains found in nibrin and the NBS phenotype suggest that this disorder is caused by defective responses to DNA double-strand breaks.

Introduction

Nijmegen breakage syndrome (NBS), a rare autosomal recessive disorder, belongs to the group of inherited human chromosomal instability syndromes that includes Bloom's syndrome, Fanconi's anemia, and ataxia telangiectasia (AT). All of these disorders are characterized by spontaneous chromosomal instability, immunodeficiency, and predisposition to cancer but have distinct cytogenetic features and sensitivities to specific DNA-damaging agents (for review, see Digweed, 1993). NBS shares a number of features in common with AT: most notably, a specific sensitivity to ionizing radiation (IR), characteristic chromosomal rearrangements in cultured lymphocytes, and a predisposition to malignancies, particularly lymphoid cancers. Based on these features and the results of earlier somatic cell complementation studies, NBS has long been classified as a variant of AT (for review, see Shiloh 1997; Wegner et al., 1998). However, NBS has been shown to be genetically distinct from AT (Saar et al., 1997) and, as demonstrated in this report, results from mutations in a novel mammalian gene.

Clinically, NBS is characterized by developmental defects, immunodeficiency, chromosomal instability, and an increased incidence of malignancies. Developmental defects typically observed in NBS patients include a severe and progressive microcephaly, growth retardation, mild to moderate mental retardation, and primary ovarian failure. Humoral and cellular immunodeficiency with recurrent respiratory infections is a consistent finding in NBS, but patients show intra- and interfamiliar variability. The immunologic characteristics of NBS encompass both developmental defects in tissues where lymphocytes develop and cellular defects in the responses of these cells to stimuli. (Wegner et al., 1998).

Chromosomal abnormalities are observed in cultured lymphocytes from NBS patients (for review, see Wegner et al., 1998). The most frequently observed cytogenetic aberrations are rearrangements involving chromosomes 7 and 14 as observed in AT patients (van der Burgt et al., 1996). The distribution of the breakpoints on these chromosomes is nonrandom and preferentially clusters around immunoglobulin and T cell receptor loci where recombination events involving double-strand breaks occur during lymphoid development. Malignancies, predominantly of lymphoid origin, occur in NBS with a high frequency and at atypically young ages. The most common tumors are B cell lymphomas (Wegner et al., 1998).

[13]To whom correspondence should be addressed.
[14]These authors contributed equally to this work.

Cultured cells from NBS patients have impaired responses to ionizing radiation, including an increased frequency of chromosomal aberrations, reduced survival in colony-forming assays (Taalman et al., 1983; Jaspers et al., 1988a), radio-resistant DNA synthesis (RDS) (Jaspers et al., 1988b; Wegner et al., 1988; Chrzanowska et al., 1995), a failure to activate cell cycle checkpoints (Seyschab et al., 1992; Jongmans et al., 1997; Antoccia et al., submitted), and a delayed up-regulation of p53 levels (Jongmans et al., 1997; Matsuura et al., 1998; Antoccia et al., submitted). All of these features are also observed in cells from patients with AT (Shiloh, 1997).

In order to understand the complex relationship between NBS and AT, cell lines from patients with these disorders have been fused and assayed for various phenotypes involving response to ionizing radiation. Complementation for RDS has been reported in AT/NBS cell hybrids (Jaspers et al., 1988a, 1988b; Wegner et al., 1988). However, complementation of RDS has also been observed in hybrids resulting from fusions of cells from different AT patients, suggesting the existence of multiple complementation groups for AT (Jaspers et al., 1988a, 1988b)—a finding that has not been borne out by mutational analysis of the *AT* gene (*ATM*) (Savitsky et al., 1995; Concannon and Gatti, 1997). Microcell-mediated transfer of a normal copy of chromosome 11 containing the *AT* gene did not complement the radiation sensitivity of NBS cells, suggesting that the gene mutated in NBS was not *ATM* (Komatsu et al., 1996). Noncomplementation was also observed in AT/NBS hybrids tested for another phenotype, radiation-induced chromosomal aberrations. This latter finding has been interpreted as suggesting that the products of the *AT* and *NBS* genes, although distinct, may interact in a common biochemical pathway or may be parts of a common protein complex (Stumm et al., 1997).

In order to identify the underlying defect in NBS, we have utilized genetic linkage analysis and positional cloning to isolate the *NBS* gene. Our previous genome-wide search for linkage in NBS families localized the gene to a 1 cM region on chromosome 8q21 (Saar et al., 1997). However, the large physical size of this region, and the small number of available NBS families with informative recombination events, limited further progress toward gene identification. In this report, we describe how linkage disequilibrium associated with a common founder effect mutation among patients of Slavic origin allowed us to narrow the *NBS* critical region to less than 300 kb. A gene in this region was found to have truncating mutations in all NBS patients. We have designated this gene *NBS1* and its product, nibrin. Biochemical characterization of the function of its product presented in the accompanying paper (Carney et al., 1998, this issue of *Cell*) reveals a clear connection between the processes of double-strand break repair and mammalian cellular responses to DNA damage.

Results

Fine Mapping through Conserved Haplotype Analysis

We previously mapped a gene for NBS to a 1 cM region on chromosome 8q21 between markers D8S271 and D8S270 (Saar et al., 1997). Based on radiation hybrid data, we estimated this region to be as large as 8 Mb, too large for positional cloning (Cerosaletti et al., submitted). However, we had also observed marked linkage disequilibrium between NBS and alleles at the microsatellite marker D8S1811 located within this minimal region and less strong linkage disequilibrium for the flanking markers D8S271 and D8S270 (data not shown). We therefore analyzed other polymorphic markers, which had been previously mapped to a YAC contig of the region (Hudson et al., 1995). All these markers also exhibited linkage disequilibrium, though they showed considerably more overlap in allelic distribution between normal and mutant chromosomes than D8S1811.

The full extent of the linkage disequilibrium only became apparent when we constructed haplotypes for these markers and compared them within our panel of 51 unrelated NBS patients, mostly of Polish or Czech origin. Five patients, of Italian, Mexican, English, Canadian, and Dutch origin, exhibited at least one unique haplotype. The remaining patients shared a common haplotype across the entire interval from D8S271 to D8S270 (Figure 1). Some patients only shared alleles at more central loci within this interval such as D8S1811 and D8S88, suggesting that ancestral recombination events had eroded the common haplotype. We hypothesized that the *NBS* gene must lie in the smallest segment of the haplotype that was shared by all patients who exhibited at least part of the common ancestral haplotype.

To refine further the extent of the shared haplotype, we identified and typed further polymorphisms from the region including microsatellites and SNPs (single nucleotide polymorphisms) detected in ESTs and cDNAs. Detailed haplotypes spanning the NBS critical region could be constructed from 38 unrelated families carrying the conserved haplotype or parts thereof. When these were arrayed based not on their descendance, but on their degree of haplotype sharing, it became apparent that a single segment flanked by the markers H4CA–H5CA was shared among all patients, independent of their geographic origin (Figure 1).

BAC Contig Construction

A BAC/PAC contig was constructed for the critical region between the markers H4CA and H5CA defined by haplotype analysis. Initially, we identified BACs for D8S88, D8S1811, D8S1724, and AFM289zb5 followed by screens for ESTs WI 8975 and StG9973. BAC ends were sequenced to generate new STSs, which were used for further STS content mapping and in walking experiments to identify further BAC clones or PAC clones. In total, 36 BACs and 22 PACs were used to construct a contig, which was estimated to span 1.2 Mb based on the long-range restriction map (data not shown). A subset of 12 BACs and PACs was used to construct the contig spanning the NBS critical region shown in Figure 2. Two known genes, calbindin (*CALB*) and 2,4-dienoyl-CoA reductase (*DECR*) could be placed on this map (Figure 2).

Transcript Detection

Transcripts were identified through two strategies: (1) All known transcripts and ESTs mapped with radiation

	D8S271	D8S1820	AFM289	BR4	H3GT	BR23	H2CA	D8S88	H3GTA	H4CA	BR11	CALB	H5CA	D8S1158	D8S1724	D8S270
F1 F	257	145	189	2	216	2	232	90	174	246	2	2		108	142	200
F7 M	257	145	189	2	216	2	232	90	174	246	2	2	189	108	142	
F12 M	257	145	189	2	216	2	232	90	174	246		2	189	108	142	200
F13 F	257	145	189	2	216	2	232	90	174	246	2	2		108	142	
F21 M	257	145	189	2	216	2	232	90	174	246		2		108	142	200
F25 M	257	145	189		216	2	232	90			2	2		108	142	200
F39 M	257	145	189		216		232	90	174	246	2			108	142	200
F17 F	257	145	189		216	2	232	90	174	246	2	2	189	108	142	200
F2 F	257	145	189	2	216	2	232	90	174	246		2		110	142	200
F21 F	257	145	189	2	210	2	236	90	174	246	2	2		108	142	200
F14 M	257	145	189	2	216	2	232	92	174	246	2			108	142	200
F13 M	257	139	189	2	216	2	232	90	174	246	2	2		108	142	
F35 M			189		216	2	232	90				2		108	142	
F35 F			189		216	2	232	90				2		108	142	
F32 M			189					90						108	142	
F32 F			189					90						108	142	
F19 M	257	145	189		216	2	232	90	174	246				108	142	198
F4 M	257	145	189	2	216	2	232	90	174	246				108	142	196
F24 M	257	145	189	2	216	2	232	90	174	246	2	2		108	142	196
F9 F	257	145	189	2	216	2	232	90	174	246	2	2		108	142	188
F3 M	257	145	189	2	216	2	232	90	174	246	2	2	189	110	142	188
F2 M	257	145	189	2	216	2	238	90	174	246		2		108	142	194
F9 M	257	145	189	2	216	2	232	92	174	246	2	2		108	142	188
F15 M	257	145	189	2	216	2	232	88	174	246	2			108	142	196
F15 F	257	145	189	2	216	2	232	88	174	246	2			108	142	196
F46 M	257		189		216		238	90	174	246			189	108	142	196
F43 F	257	137	189	2	216	2	234	90	174	246	2	2	189	108	142	188
GM7078 ?	257	139	189	2	216	2	232	90	174	246	2	2		108	142	196
F18 M	257	145	189	2	216	2	232	90	174	246	2	2		108	146	188
F44 F	257	145			216	2	232	90	174	246				108	140	192
F8 M	257	145	189	2	216	2	232	90	174	246	2	2	189	83	138	196
F12 F	257	145	189	2	216	2	232	90	174	246		2	185	110	142	200
F47 ?	257		189		216		232	90	174	246			185	110	142	188
F33 F	257	145	189	2	216	1	232	90	174	246	2	2	185	106	146	196
F6 F	255	145	189	2	216	2	232	90	174	246	2	2	185	106	146	184
F47 ?	261		189		210		234	90	174	246	2		185	106	148	200
F10 M	259	145	189		216	2	232	90	174	246				108	142	200
F10 F	259	145	189		216	2	232	90	174	246				108	142	200
F20 C	259	145	189		216		232	90	174	246				108	142	200
F34 ?	259	145	189		216	2	232	90	174	246	2	2		108	142	
F22 ?	259	145	189		216	2	232	90	174	246	2			108	142	200
F29 M	259	145	189					90		246				108	142	
F29 F	259	145	189					90		246				108	142	
F30 F	259	145	189					90		246				108	142	200
F14 F	255	145	189	2	216	2	232	90	174	246	2			108	142	200
94P126 ?	255		189		218		232	90	174	246	2		189	102	142	200
F7 F	259	145	189	2	218	2	232	90	174	246	2	2	189	108	142	
F4 F	255	145	189	2	216	2	232	90	174	246				108	142	188
F16 M	259	145	189		216	2	232	90	174	246				108	142	188
F16 F	261	145	189		216	2	232	90	174	246				108	142	188
F19 F	259	145	189		216	2	232	90	174	246				108	142	196
F30 M	259	145	189					90		246				108	142	188
F44 M	259	145			216	2	232	92	174	246				108	142	188
F22 ?	255	145	189		216	2	232	92	174	246	2			108	142	188
F18 F	259	139	189	2	216	2	232	90	174	246	2	2		108	142	200
F39 F	259	139	189		216		232	90	174	246	2			108	142	200
F26 M	255	139	189		216	2	232	90	174	246	2			108	142	200
F26 F	255	139	189		216	2	232	90	174	246	2			108	142	200
F34 ?	261	139	189		216	2	232	90	174	246	2	2		108	142	
5230 ?	255	141	189	2	216	2	232	90	174	246	2	2	189	108	142	200
F1 M	259	139	189	2	216	2	232	90	174	246	2	2		108	142	198
F17 M	257	141	189	2	216	2	232	90	174	246	2	2	189	108	142	198
5230 ?	255	139	189	2	216	2	232	90	174	246	2	2	189	108	142	198
F25 F	255	141	189		216	2	232	90			2	2		108	140	198
F41 F	255	139	189	2	216	2	232	88			2	2	185	106	142	186
G25-1-1 C	259	137	191	2	216	2	232	90	174	246	2	2		108	142	200
F3 F	257	141	191	2	216	2	232	90	174	246	2	2	189	108	142	202
94P126 ?	255		191		218		232	90	174	246	2		189	108	142	200
F33 M	255	145	191	1	196	2	230	90	174	246	2	2	189	108	142	200
F46 F	257		189		218		232	86	174	246			189	108	142	200
F41 M	255	139	191	1	216	1	232	94			2	2	189	108	142	184
F43 M	257	145	187	2	210	2	236	76	174	246	2	2	189	108	142	194
GM7078 ?	257	143	189	1	218	1	232	98	184	254	2	2		108	142	188
F24 F	267	141	189	2	210	2	236	90	176	248	2	2		108	142	200

Figure 1. Haplotype Analysis in NBS Patients and Families

Most likely, haplotypes for markers from the interval D8S271–D8S270 containing the *NBS1* gene were constructed for all NBS patients. Haplotypes from 38 patients showing large similarities were ordered based on their degree of overlap. Marker order was derived from our BAC/PAC contig and from the Whitehead YAC contig WC8.8 (Hudson et al., 1995). NBS families are numbered, and parental origin of chromosomes, where known, is indicated (e.g., F1 F = family one, paternal chromosome; F, father; M, mother). When only material from the patient was available, a question mark indicates the unknown parental origin. Patients F20 and G25-1-1 are from consanguineous marriages and therefore only one haplotype (labeled C) is given. The haplotype showing the most common alleles on NBS chromosomes was designated as the common haplotype. Alleles showing deviation from this haplotype are shaded. When two adjacent microsatellites or one single nucleotide polymorphism and one adjacent microsatellite deviated from the common allele, we assumed an ancestral recombination event had occurred (boxed segments). All other deviations were regarded as possible mutations of microsatellite or SNP alleles. The segment of the haplotype including the SNPs at BR1 (part of the *NBS1* gene) and *CALB* (calbindin) is shared by all patients. Two haplotypes identify H4CA as the proximal border, and six chromosomes identify H5CA as the distal border of the *NBS1* critical region. Based on the long-range restriction map (Figure 2), this critical region was estimated to be less than 290 kb.

hybrids by Schuler et al. (1996) to the interval D8S270–D8S271, or to the two immediately adjacent intervals, were mapped on the BAC/PAC contig. In total, nine ESTs were mapped to specific genomic clones by PCR amplification. (2) Based on the genomic sequence obtained from low-redundancy sequencing of the entire BAC/PAC contig, additional, previously unmapped ESTs were identified through repeated database searches. By these approaches, 31 ESTs were identified, which were later consolidated into 21 cDNA contigs (M. P. et al., unpublished data). Sequences were verified against the genomic sequence to identify exons and introns and were investigated for putative open reading frames and homology to other species.

Mutation Detection

In order to search for mutations, we extracted mRNA from lymphoblastoid cell lines from 14 patients homozygous for the conserved haplotype, and one patient that was heterozygous, and amplified overlapping cDNA fragments of 300 bp average size for all transcripts identified in the 1.2 Mb region. When genomic sequence information was available for a given transcript, we also amplified exonic fragments from genomic DNA from additional patients for whom lymphoblastoid cell lines were not available. All PCR fragments were analyzed by SSCP and/or direct sequencing. Eight genes was screened for variation. Polymorphisms in three cDNA contigs, BR1, BR4, BR23, and one known gene, *CALB*, were identified based on their presence in both patients and controls. These polymorphisms were used as markers to refine further the haplotyping (Figure 1).

In one cDNA contig, BR7, we identified an aberrant banding pattern by SSCP in a cDNA fragment amplified from all patients with the conserved haplotype but none of the controls. Sequencing of this product revealed a homozygous 5 bp deletion (Figure 3) predicted to result in a frameshift and in premature termination 15 aa downstream. This mutation was present on all chromosomes bearing the conserved haplotype or parts thereof. It was not detected in any of 50 normal control individuals nor on any of 28 normal (untransmitted) chromosomes from NBS parents examined, further suggesting that this was a causative mutation for NBS.

Identification of the *NBS* Gene

After the initial identification of a common truncating mutation in BR7, the transcript was further extended in 5′ direction and linked to the 2.6 kb BR1 cDNA contig, which contained a poly (A) tail, defining the 3′ end of the gene. The entire cDNA sequence (Figure 4) of 4386 bp contains an ORF of 2277 bp. The first ATG at position 26 of this sequence was assumed to be the translation initiation site. The encoded protein of 754 aa has a predicted molecular mass of 85 kDa. We termed the gene *NBS1*, and its protein product, nibrin. The nucleotide sequence of a genomic contig of 66 kb containing the entire *NBS1* gene was determined. Comparison of the genomic sequence to that of the cDNA allowed us to define the exon–intron organization of the gene. In total, 16 exons were identified, which, together with introns, spanned over 50 kb. Fluorescent in situ hybridization

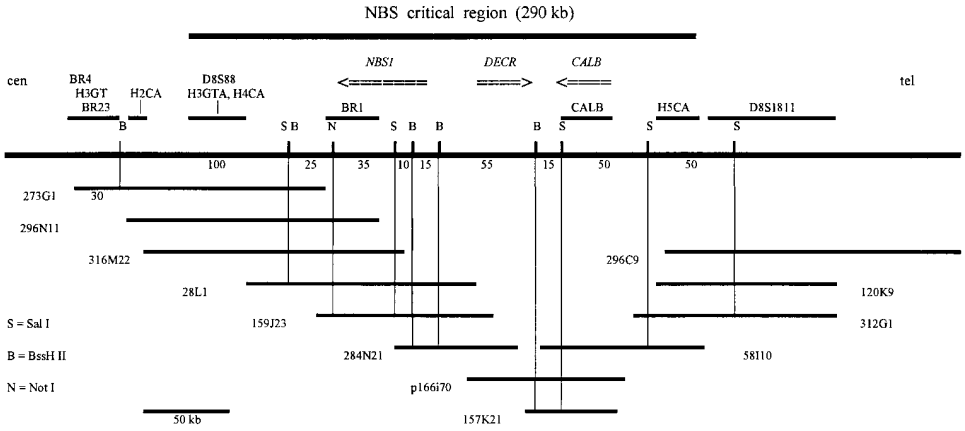

Figure 2. BAC/PAC Contig of the NBS Critical Region

BAC and PAC contig of the NBS critical region (marked with bar) based on the haplotype analysis in Figure 1. BAC clones are identified by their coordinates; the only PAC clone is p166i70. The approximate position of the polymorphic markers is indicated by bars. Position of D8S88, H3GTA, and H4CA could not be differentiated. For details, see Figure 1. Vertical lines indicate presence of sites for rare cutting restriction enzymes (S, SalI; B, BssHII; N, NotI); numbers indicate sizes in kilobases. Cen, centromere; tel, telomere. Gene positions are indicated by arrows.

(FISH) using a directly labeled BAC clone containing the *NBS1* gene as a probe localized the gene to 8q21.13–q21.3 (data not shown).

Northern blots containing mRNA from 16 different tissues were probed with a 576 bp fragment from the coding region of the *NBS1* gene. Transcripts of 2.4 and 4.4 kb were observed in all tissues (Figure 5). The presence of the smaller 2.4 kb transcript was unexpected. However, in the 3′ untranslated region of the cDNA, two potential polyadenylation signals were found at positions 2440 and 4386 (Figure 4). Comparison of ESTs in the database containing the 3′ end of the transcript confirmed that both polyadenylation signals are used to generate the alternative transcripts. Densitometry and phosphorimaging of Northern blots were used to quantitate transcript levels for *NBS1* relative to a *GAPDH* control. Three tissues, spleen, testis, and ovary, had approximately 2-fold more transcripts than other tissues. The 4.4 kb transcript predominated in most tissues except testis, where the 2.4 kb transcript was more common. No significant increase in transcript levels was observed in fibroblasts after irradiation with 5 Gy (data not shown).

Sequence comparisons of nibrin with other protein sequences in the database failed to identify any global similarities. Comprehensive sequence comparisons revealed two domains in the amino-terminal region, a forkhead–associated domain (FHA) (Hofmann and Bucher, 1995), residues 24–100, and a **br**east cancer **c**arboxy-**t**erminal domain (BRCT) (Bork et al., 1997), residues 105–190. Both domains have been found separately in DNA damage-responsive cell cycle checkpoint proteins; their adjacent localization in nibrin, though, is remarkable (Figure 6).

Mutation Screening

All NBS chromosomes with the conserved Slavic marker haplotype were found to bear the 657del5 mutation, suggesting a founder effect for this mutation. For subsequent mutation analysis, a set of intronic primers flanking each of the 16 exons was designed from the genomic sequence obtained through sequencing of the BAC contig. These primers were used to screen the additional five patients who had at least one chromosome that did not carry the 657del5 mutation or the conserved haplotype. Mutations were identified in all of these patients, most being small insertions or deletions (Table 1). All mutations were predicted to cause premature truncation downstream of the FHA and BRCT domains.

Thus far, all NBS patients from families with genetic linkage to 8q21 have mutations in the *NBS1* gene. This includes 46 patients homozygous for the common 657del5 mutation, including the first patient described (Weemaes et al., 1981), 2 patients heterozygous for 657del5 and a second mutation, and 3 patients homozygous each for unique NBS mutations (Table 1). We also detected three polymorphisms (Table 1) including one nonconservative amino acid substitution at position 185 (glutamine for glutamic acid). Control probands of German origin who were homozygous for each of these alleles were identified.

Discussion

Haplotype Mapping in Nonisolated Populations

One of the major obstacles for positional cloning is mapping the trait of interest to a sufficiently small region, usually less than 1 Mb, allowing for efficient gene identification with current techniques. Linkage disequilibrium methods have been widely used in populations isolated due to geographic reasons, such as Finns or French-Canadians, or due to religious and cultural reasons, such as Jews or the Amish, to proceed from an initial finding of linkage to a region of several cM down to a few hundred kilobases containing the gene. Our finding of a shared haplotype in NBS patients from various populations from central Europe, predominantly Polish and Czech, came as a surprise, because neither marked cultural nor geographic nor religious separation is evident. All patients from these two populations studied share the same founder mutation, suggesting that this

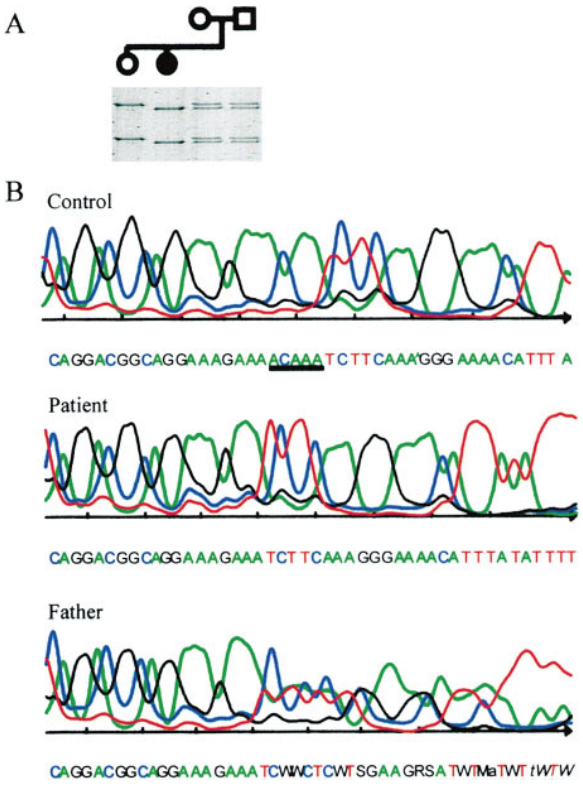

Figure 3. Common NBS Mutation

Detection of the common 657del5 mutation of probable Slavic origin.
(A) SSCP pattern of exon 6 of Polish NBS family F24.
(B) Segment of genomic sequence of exon 6 in a control DNA, the patient, and the father from family F24. The 5 bp deleted in the patient is marked with a bar in the control sequence. In the sequence of the heterozygote father, a frameshift in the sequence starting at the deletion site can be seen.

mutation is of Slavic origin. The observation of the same mutation and haplotype in German, Dutch, American, and even one Greek patient is testimony to the high degree of admixture in European populations.

Most recessive genetic disorders studied to date in European populations have shown a plethora of different mutations and haplotypes. The best studied exception to this rule is cystic fibrosis (CF), where a major mutation, the dF508 mutation, is found in high frequency in Caucasian populations worldwide. The current prevalence of the dF508 mutation reflects both the age of this mutation, which is estimated to have occurred more than 60,000 years ago (Morral et al., 1994), and the likelihood that CF carriers have had a selective advantage sometime in the past (Gabriel et al., 1994). In CF, linkage disequilibrium is barely detectable at a distance of more than 300 kb. This is not surprising considering the number of generations estimated to have passed since the original mutational event. Among NBS patients bearing the 657del5 mutation, significant linkage disequilibrium can be detected at more than 0.5 cM (1.5–2 Mb distance) from the *NBS1* gene, clearly indicating that this is a much more recent mutation. The limited incidence of the 657del5 mutation in the general population as compared to the CF mutation dF508 excludes selective advantage in heterozygotes, in accordance with the different nature of the basic defect.

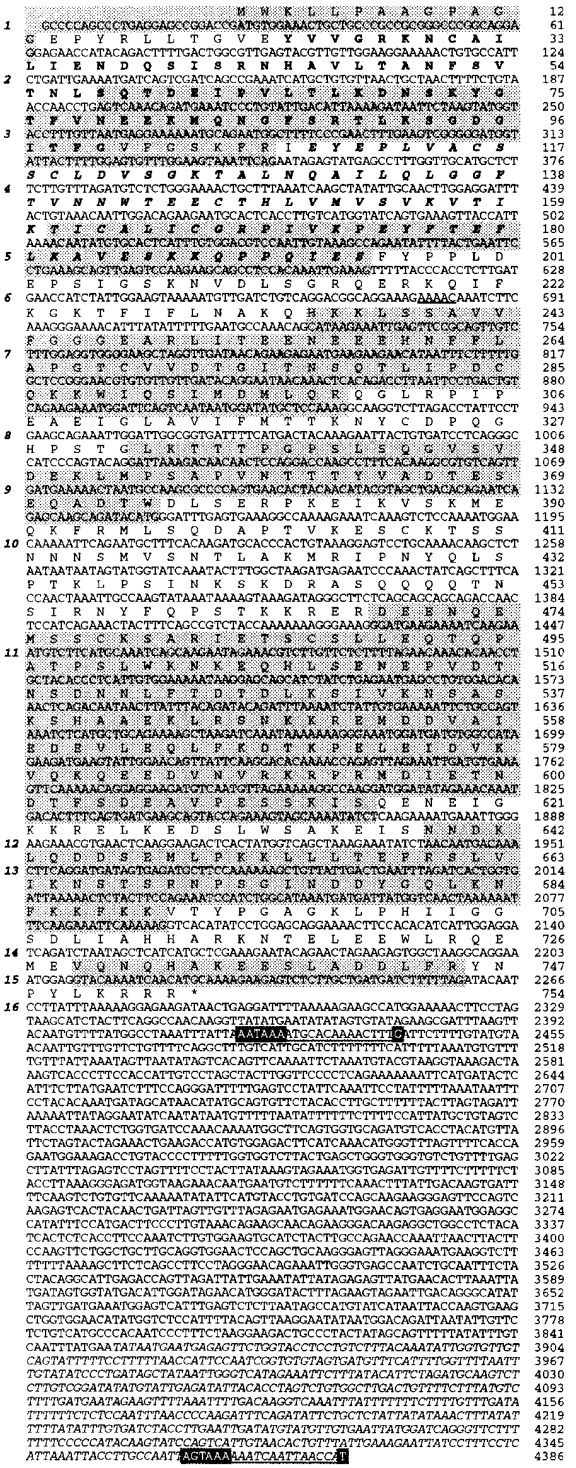

Figure 4. Nibrin cDNA Sequence

Underlined, mutation 657del5; gray shaded, exons with odd numbers; bold, FHA domain; bold italic, BRCT domain; italic, L1MC/D genome-wide repeat; black shaded, polyadenylation signal and site.

Gene Identification

Using various known STSs for PCR screening of BAC/PAC libraries and several walking steps, we were able to obtain a contiguous array of clones covering 1.2 Mb.

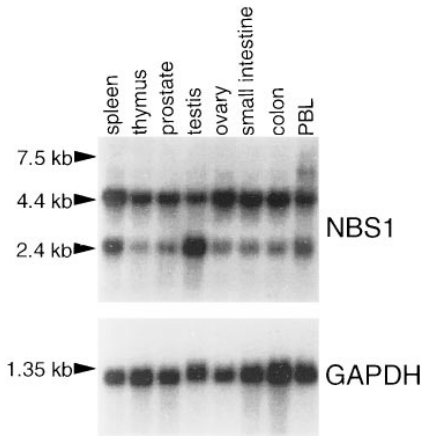

Figure 5. Northern Blot

Expression of the *NBS1* gene in multiple human tissues. A commercial multiple tissue Northern blot was sequentially hybridized with probes for *NBS1* and GAPDH (as a control for loading). Tissue of origin for RNA is indicated above. Migration of size markers is indicated at left.

Low-redundancy sequencing (skimming) of a selection of these clones allowed positioning of a large number of previously unmapped ESTs onto the contig. Through sequencing of the corresponding cDNA clones for these ESTs, a total of 21 cDNA contigs could be assembled. These various cDNA contigs extended from several kilobases in size to near completion (M. P. et al., unpublished data). The *NBS1* gene is represented by 33 different ESTs, a testimony to the completeness of public EST databases, at least for transcripts expressed in a wide variety of tissues. We also carried out exon trapping on selected BAC and PAC clones, which successfully identified two exons of *NBS1*. However, the skimming strategy in conjunction with detailed sequence annotation and exhaustive database searches proved the most successful in positional cloning of the *NBS1* gene.

NBS Mutations

Mutation screening of the *NBS1* gene identified a total of six distinct mutations in various NBS patients, summarized in Table 1. The vast majority of the patients are homozygous for the common deletion mutation 657del5, which is found exclusively on the conserved Slavic haplotype. Three other mutations are deletions of 1 or 4 bp, and one was an insertion of a single nucleotide. All are predicted to cause a frameshift and thus premature truncation. One further mutation, 976C>T, is a point mutation creating a stop codon (Q326X) in exon 8 in a Dutch patient who is homozygous for this mutation. In the accompanying manuscript, Carney et al. demonstrate that the nibrin protein is undetectable by Western blotting in five NBS patients, four of whom are homozygous for the 657del5 mutation and a fifth who is heterozygous for 657del5 and 1142delC. Thus, it seems likely that some or all of these truncating mutations result in null alleles and that the majority of NBS patients will lack any functional nibrin protein. This collection of nonsense mutations in NBS patients represents compelling evidence that we have indeed identified the *NBS* gene.

Truncating mutations, particularly if they result in the absence of even altered protein, do not provide significant insights with regard to functional domains of the protein of interest. Although we speculate that all of the truncating mutations we have detected in NBS result in null alleles, it is of interest that all such mutations we have detected occur downstream of the FHA and BRCT domains in nibrin. In this study, we investigated only patients showing the full NBS phenotype. However, even among this highly selected group we observed genetic heterogeneity (Cerosaletti et al., submitted) and therefore termed the locus *NBS1*. It is possible that apart from null mutations other mutations may exist that reduce nibrin levels or lead to inactivation and hence to a milder phenotype. In AT, a characteristic of these "variants" is a later onset and slower progression of the disease (reviewed by Shiloh, 1997).

Nibrin Function

The hallmarks of NBS are radiation sensitivity, immunodeficiency, and chromosomal instability. This unusual combination of phenotypes is the characteristic manifestation of defective DNA double-strand break (DSB) repair, as recently reviewed by Hendrickson (1997). The exposure of mammalian cells to IR induces lesions in chromosomal DNA such as strand scission, single-strand breaks, DSBs, and base cross-links. In particular, DNA DSBs appear to be the predominant cytotoxic lesions, since even a single unrepaired DNA DSB can be a lethal event. Similarly, the development of the mammalian immune system is dependent on a site-specific DNA recombination process in creating immunoglobulin and T cell receptor genes. Formation of DNA DSBs is an essential step in the V(D)J-reaction mechanism. Thus, the repair of DNA DSBs is an integral feature of IR sensitivity and of V(D)J recombination (Hendrickson, 1997). In addition, DNA breaks regularly occur in meiotic recombination, and it is well documented that the ATM protein associates with meiotic prophase chromosomes. In $ATM^{-/-}$ mice, the chromosomes fragment in early pachytene, leading to infertility. Gonadal dysfunction in AT patients and ovarian failure in NBS probands could thus be a reflection of a defect in meiotic recombination (reviewed by Shiloh, 1997).

The identification of nibrin as the *NBS1* gene product thus implies its role in the mammalian response to DNA double-strand breaks. This is corroborated by the identification of protein domains that have been previously found in DNA damage-responsive cell cycle checkpoint proteins. In the amino-terminal region, a forkhead-associated domain is present (Figure 6). This domain, described by Hofman and Bucher (1995), is possibly involved in mediating phospho-ser/thr-specific interactions and has been found in *Saccharomyces cerevisiae DUN1* and *RAD53*, two protein kinases linking the S phase checkpoint to DNA damage repair and in *Schizosaccharomyces pombe* cds1, a kinase acting in the S phase checkpoint. The breast cancer carboxy-terminal domain, recently described by Bork et al. (1997), is found in a variety of diverse proteins whose unifying theme seems to be participation in DNA damage-responsive cell cycle checkpoints.

Database comparisons with the nibrin sequence failed

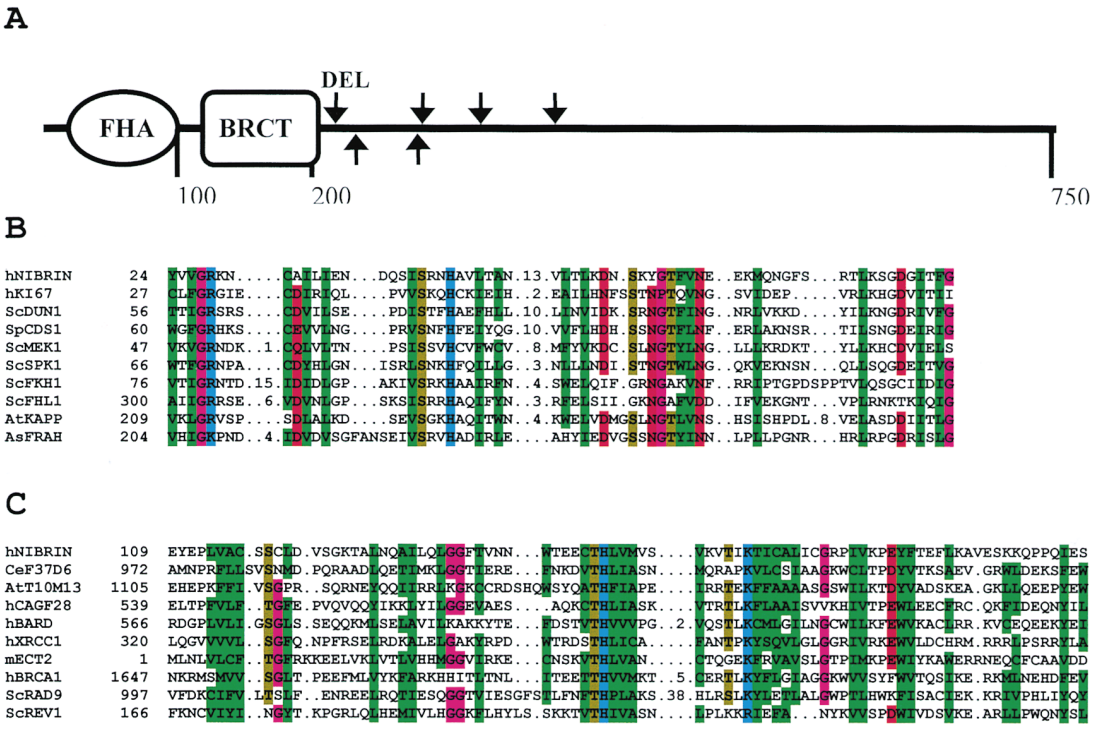

Figure 6. FHA and BRCT Domains in Nibrin

(A) Localization of domains and of mutations (arrows) detected in patients with Nijmegen breakage syndrome. The common 5 bp deletion 654del5 of Slavic origin is tagged (DEL).

(B and C) Multiple sequence alignments with known FHA (Hofmann and Bucher, 1995) and BRCT (Bork et al., 1997) domains. Coloring of conserved positions (at most, three deviating amino acids): green, hydrophobic (FILMVTAC); red, acidic (DEQN); blue, basic (HKR); magenta, glycine (G); ochre, serine or threonine (S, T). Sequences are denoted by species identification prefixes (h, human; m, mouse; At, *A. thaliana*; Sc, *S. cerevisiae*; Sp, *S. pombe*; As, *Anabaena Sp.*; Ce, *C. elegans*) and by protein acronyms (the kinase-associated protein phosphatase KAPP; the forkhead and -like proteins FKH1 and FHL1; the protein kinases SPK1, DUN1, and MEK1, which all have been described to act in the nucleus and to respond to signals related to DNA replication and repair; the protein kinase CDS1 known to act in the S phase checkpoint; the antigen KI67, expressed in a cell cycle–dependent manner; the FRAH protein involved in differentiation from vegetative cells to heterocysts; conceptual translations of the cosmids F37D6.1 and T10M13.12; the CAG trinucleotide repeat containing cDNA CAGF28; the BRCA-associated RING finger domain protein BARD; the DNA repair proteins XRCC1 and REV1; the oncoprotein ECT2; the breast cancer susceptibility type 1 protein BRCA1; the radiation sensitive checkpoint protein RAD9). Numbers in the alignment denote amino acids omitted from it.

to detect any global homology to other known proteins. This was surprising, as other proteins involved in DSB repair have well conserved homologs in *S. cerevisiae*, such as MRE11 and RAD50 from the RAD50 complex (Petrini et al., 1995; Dolganov et al., 1996) or the heterodimeric Ku proteins from the DNA–PK complex (Troelstra and Jaspers, 1994; Wang et al., 1998). DNA–PK itself, though, and the other known components of that complex seem, similarly to nibrin, not to be conserved in yeast. However, biochemical analyses suggest that nibrin may be the mammalian equivalent of the *S. cerevisiae* XRS-2 protein, which forms part of the Rad50 complex (Carney et al., 1998). Thus, lack of primary sequence conservation even in such an essential pathway as DSB repair may not preclude functional conservation.

Possible Interaction between Nibrin and ATM

NBS and AT have significant overlap in their clinical and biochemical features, suggesting that the nibrin and

Table 1. NBS Gene Mutations and Polymorphisms

Name	Nucleotide Change	Exon	Consequence	Origin
Mutations				
657del5	667–661delACAAA	6	Frameshift	Slavic
698del4	698–701delAACA	6	Frameshift	English
835del4	835–838delCAGA	7	Frameshift	Italian
842insT	842–843insT	7	Frameshift	Mexican
1142delC	1142delC	10	Frameshift	Canadian
976C>T	C > T at 976	8	Q326X	Dutch
Polymorphisms				
553G/C	G > C at 553	5	Glu > Gln at 185	—
1197T/C	T > C at 1197	10	—	—
2016A/G	A > G at 2016	13	—	—

ATM proteins may function in a common pathway. Although these disorders differ in key diagnostic features, ataxia and telangiectasia in the case of AT and microcephaly in the case of NBS, these discrepancies could well be explained by differences in the timing or tissue specificity of expression of their respective genes early in development. Both disorders are characterized by chromosomal translocations arising at sites of V(D)J rearrangement, gonadal failure, and sensitivity to ionizing radiation. Based on these observations, AT has long been theorized to arise from a defect in the processing of double-strand breaks in DNA (Hanawalt and Painter, 1985; Meyn, 1995). In the accompanying manuscript, Carney et al. provide evidence that nibrin can form complexes with at least two other proteins, hRad50 and hMRE11, that are believed to play a role in double-strand break repair. This provides further support for the idea that deficiency in either nibrin or ATM, as occurs in NBS and AT, respectively, disrupts a common pathway that functions to sense or repair double-strand breaks.

Experimental Procedures

Patients' RNA and DNA Samples

Fifty-one unrelated NBS families, mainly of Polish, but also Czech, German, Dutch, Italian, Mexican, Spanish, UK, Canadian, and US origin have been collected for this study. The diagnosis of NBS in all families was made as previously described (Saar et al., 1997; Cerosaletti et al., submitted). Blood samples were obtained from the families under informed consent. DNA was extracted from whole blood, using a Nucleon II Kit (Scotlab), according to the manufacturer's instructions. Total RNA was extracted from lymphoblastoid cell lines that had been established from 14 NBS patients using the phenol-chloroform procedure (Trizol, Life Technologies).

Haplotype Analysis

Microsatellite markers from the interval D8S271–D8S270 on chromosome 8q21, namely AFM289zb5, D8S88, and D8S1724, were analyzed as previously described (Saar et al., 1997) using primer sequences deposited in GDB. Newly ascertained microsatellites based on the genomic sequence derived from the BAC/PAC contig were designated H3GT, H2CA, H3GTA, H4CA, and H5CA and amplified using standard conditions—5 min 94°C, 30 cycles (30 s 94°C, 30 s 55°C, 30 s 72°C) 7 min 72°C. Single nucleotide polymorphisms were amplified under the same conditions and detected through SSCP analysis as described under mutation detection.

The order of markers previously described in YAC contig WC8.8 of the Whitehead Institute (Hudson et al., 1995) was verified through amplification from the three most relevant YACs, 829G6, 820C9, and 952E8. We considered as true ancestral recombination events only those where the departure from the common haplotype was at least in two adjacent microsatellites or single nucleotide polymorphisms. Variations of a single repeat unit from the common allele in isolated microsatellites, as is the case in haplotypes F2F and F14M in Figure 1, were interpreted as ancestral mutational events in that microsatellite.

Primers

The following primers were used in haplotype analysis: H3GT F, 5′-CCGCCCTGTGATGACCTAGA-3′; H3GT R, 5′-GACAGAGCGAGACTCCGTCT-3′; H2CA F, 5′-GCCAACCTATCCTTTGAGAC-3′; H2CA R, 5′-GGGTACATCAGCAAGAAGTC-3′; H3GTA F, 5′-AATAGGCCATGTGGTAGCTC-3′; H3GTA R, 5′-AGGAGTTGATTGTACCGGTG-3′; H4CA F, 5′-TTAAGGAGTTGATTGTACCG-3′; H4CA R, 5′-AGTGGAGTAGAATAAGGTGA-3′; H5CA F, 5′-CAAAGTGTAAAGCACAGTAG-3′; H5CA R, 5′-TCAAGCTGATGTGAGAAAGT-3′; BR1 F, 5′-GTAAACAGAAGCAACAGAAG-3′; BR1 R, 5-GGCAAGGTAATTTAATGAGG-3′; BR4 F, 5′-CGCTAGTTACTGTATTACTG-3′; BR4 R, 5′-ATGAAGCAAGTCACTACAAC-3′; BR23 F, 5′-CCCTATCAAATTGGTGCTAT-3′; BR23 R, 5′-GCTAGGTCGAAGAAATAACT-3′; CALB F, 5′-AGAACTCTGGAGGAACGCTG-3′; and CALB R, 5′-AGGGCAAAGAATGGGAAGGG-3′.

BAC Contig

DNA pools from a human BAC library (Research Genetics, Hunstville, AL) were screened by PCR, as described above, for the microsatellite markers D8S88, AFMzb289, D8S1811, and D8S1724, and for ESTs previously assigned to this region (Schuler et al., 1996)—A006J10, A005L21, WI-8975 (*CALB*), and stG9973 (*DECR*). Primers corresponding to these ESTs and PCR conditions were available on the World Wide Web site at http://www.ncbi.nlm.nih.gov/SCIENCE96/. A human PAC library (Genome Systems, Inc.) was also screened for the ESTs st69973 and A006J10.

BAC and PAC clone DNA was extracted using Qiagen Plasmid Midi Kit, as recommended by the manufacturer. BAC and PACs were sized and restriction mapped by digestion with NotI, SalI, BssHII, and MluI (New England Biolabs), followed by pulsed-field gel electrophoresis (PFGE) on a Rotaphor Type 5 apparatus (Biometra). BAC and PAC ends were sequenced with T7 and Sp6 primers using Cycle Sequencing Kit (Pharmacia) on an automated DNA Sequencer (ALF, Pharmacia).

Fluorescence In Situ Hybridization (FISH)

Chromosome preparations were obtained from phytohemagglutinin-stimulated blood cell cultures by standard harvesting procedures. Isolated BAC DNA was labeled with Cy3-dCTP (AMERSHAM) by standard nick translation procedure (GIBCO BRL Nick Translation System). The labeled DNA samples (1 μg) were ethanol precipitated with sonicated herring sperm DNA (10 μg), *Cot-1* DNA (10 μg), and dissolved in 40 μl hybridization mixture (50% deionized formamide, 2× SSC, 10% dextran sulfate). Chromosomal in situ suppression (CISS) hybridization was performed following standard protocols (Lichter and Cremer, 1992). Signal detection and imaging were achieved using a LEICA DMRB/E photomicroscope and the Cytovision system (Applied Imaging).

Transcript Detection

Primers for ESTs previously reported to map to the interval D8S273–D8S270 and D8S270–D8S257 (Schuler et al., 1996) were obtained from Research Genetics. All ESTs were typed on our BAC/PAC contig and on YACs 829G6, 820C9, and 952E8 (Hudson et al., 1995) by PCR amplification as described above. Clones for ESTs mapped to the region were obtained from the German resource center (RZPD) and were entirely sequenced as described.

Mutation Detection

First-strand cDNA was synthesized from 1–2 μg total RNA with MMLV reverse transcriptase and random hexamer primers (Life Technologies) in a final volume of 20 μl (10 min 20°C, 40 min 42°C, 6 min 98°C). Three microliters of this product was used for PCR amplification. Specific primers for all transcripts were designed, and overlapping cDNA fragments suitable for SSCP analysis were amplified. When genomic sequences were available for a given transcript, we also amplified from genomic DNA of NBS patients, using exon-flanking primers. For all amplified fragments, SSCP analysis was performed (Orita et al., 1989). Aliquots (3–5 μl) of PCR products were mixed with an equal volume of loading buffer, denatured for 5 min at 95°C, chilled on ice, and loaded on 12% nondenaturing polyacrylamide gels and electrophoresed under conditions described elsewhere (Savov et al., 1992). In parallel, samples from two controls and two parents were always run for comparison. The gels were scanned for aberrant migration after staining with Vistra Green on a FluorImager, and the signals were analyzed with the ImagequaNT software (Molecular Dynamics). All samples that showed an aberrant SSCP shift were directly sequenced. After identification of the common mutation and the genomic organization of the *NBS* gene, flanking primers were designed for all 16 exons and the remaining NBS patients screened for mutations.

Primers

The following primers were used for mutation screening: Ex1 F, 5′-TCATCCAAGGCAGCCTGCGT-3′; Ex1 R, 5′-TGCCATACAGCGTACTCGCC-3′; Ex2 F, 5′-CTTTGATAGCCTTCAGTGAG-3′; Ex2 R, 5′-CTCTCTCTCACATACAAACC-3′; Ex3 F, 5′-CAGTAATTGTTGTCTGC

CGT-3′; Ex3 R, 5′-AGGATTTGGCTGAAACAAAG-3′; Ex4 F, 5′-GCT TAATGATGAGGAACTGA-3′; Ex4 R, 5′-CCTAAATGGTATACAAA GGG-3′; Ex5 F, 5′-TTATGGATGTAAACAGCCTC-3′; Ex5 R, 5′-TAC CGAACTATAACACAGCA-3′; Ex6 F, 5′-CAGATAGTCACTCCGTTT ACAA-3′; Ex6 R, 5′-ATGAATAGGCCAGTTATCACAG-3′; Ex7 F, 5′-TCAAGAAGTAGCACCAAGTC-3′; Ex7 R, 5′-AATTGCTTGAAC CCAGAAGG-3′; Ex8 F, 5′-GAGGTTGCTTTATCTTGACA-3′; Ex8 R, 5′-CCCTAGCAAGTATATAGATA-3′; Ex9 F, 5′-CTTAGCATGGTATAG TCTAA-3′; Ex9 R, 5′-CTCAAGAGACAACCTGATAA-3′; Ex10 F, 5′-TGCTTTCTTGGGATGGTAAA-3′; Ex10 R, 5′-GCAGAAGCATAC TTAATCAG-3′; Ex11 F, 5′-ATGGTTACTTAGCTGTGTTC-3′; Ex11 R, 5′-TAATGGATGCTCATACTGTC-3′; Ex12 F, 5′-ATGCCTGGTCAT ACATAACA-3′; Ex12 R, 5′-AATTGATGAGATGACAGTCC-3′; Ex13 F, 5′-AGATTCCCAAATGACAAGTG-3′; Ex13 R, 5′-AGTTCATATCCTT CCTAGAG-3′; Ex14 F, 5′-AACATCTTTGGCACTTATGC-3′; Ex14 R, 5′-AGAAGAATTTGCTTGAAGGC-3′; Ex15 F, 5′-CTATTGGTTGTCT TTGAGTG-3′; Ex15 R, 5′-ATTTCACACAATTCGGGAAC-3′; Ex16a F, 5′-TCATTCCCATCCTATTTGCC-3′; Ex16a R, 5′-TGGAAGGGTGACT TTAGTCT-3′; Ex16b F, 5′-AGGTAAAGACTAAAGTCACC-3′; Ex16b R, 5′-TGTTTGATGAAGTCTCCACA-3′; Ex16c F, 5′-AGTACTAGA AACTGAAGACC-3′; Ex16c R, 5′-ATTTGGAAGGTGAGAGTGAT-3′; Ex16d F, 5′-GTAAACAGAAGCAACAGAAG-3′; and Ex16d R, 5′-GGCAAGGTAATTTAATGAGG-3′.

Northern Blot Analysis

A probe containing nucleotides 704–1279 of the *NBS1* gene was amplified from a cDNA clone, radio-labeled by incorporation of [α^{32}P]dCTP and [α^{32}P]dATP, and hybridized overnight at 42°C in 50% formamide to human multiple tissue poly $(A)^+$ Northern blots (Clontech). The blots were washed two times for 20 min in 2× SSC/0.1% SDS at 42°C and one time for 20 min in 0.2× SSC/0.1% SDS at 55°C. Blots were then stripped by washing in 0.01× SSC/0.01% SDS at 65°C and hybridized with a radiolabeled GAPDH probe as a control for RNA loading.

Sequencing

The BACs and PACs were sequenced by the "shotgun method" as described previously (Platzer et al., 1997). For low-redundancy analysis ("skimming"), about 600–800 sequencing reads per 100 kb of human insert were obtained. In order to complete the sequence of selected clones, the number of reads was raised to about 2500 per 100 kb.

Computer Analysis

Homology searches against databases were performed with BLAST (version 1.4; Altschul et al., 1990) and FASTA (version 2.0; Pearson and Lipman, 1988). Genome-wide repeats were identified with the REPEATMASKER program (A. F. A Smit and P. Green at http://ftp.genome.washington.edu/RM/RepeatMasker.html). FHA and BRCT domains in nibrin were identified using a new method for iterative database searches and construction of consensus strings (Beckmann et al., 1998). Corroborative profile searches at ISREC's ProfileScan Server (http://ulrec3/unil.ch/software/profilescan.html) established statistical significance for the presence of the FHA domain, whereas the BRCT domain was cross-validated using MACAW (version 2.0.5; Schuler et al., 1991).

Acknowledgments

We are greatly indebted to all patients for their generous participation in this study and to Prof. R. D. Wegner (Berlin) for his earlier contribution to this work. We thank Dr. P. Maraschio (Pavia), Prof. H. H. Ropers (Berlin), Dr. V. M. Der Kaloustian and A. Elliott (Montreal), and Dr. Petersen (Athens) for making patients' cell lines available; and Dr. H. Neitzel (Berlin) for establishing lymphoblastoid cell lines. We also thank Mohsen Karbasyan, Susanne Fabisch, Hella Ludewig, Evelyn Micaelis, Nicole Steinlein, Doreen Stoetzer, Soeren Geist, Lindsey Johnson, Patsy Byers, Jocyndra Wright, Anette Quaiser, and Antje Soyke for expert technical assistance and Prof. Jens Reich (Berlin) for critical reading of the manuscript. This work was supported by grants from the National Institutes of Health (CA57569) to P. Concannon and from the Deutsche Forschungsgemeinschaft to K. Sperling, M. Digweed, and A. Reis. N. J. Nowak and P. R. Cooper were supported by grants from the National Institutes of Health (HG00333 and CA63333) to T. B. Shows. The Mikrosatellitenzentrum is supported by a grant-in-aid from the German Ministry of Research to A. Reis.

Received March 18, 1998; revised April 8, 1998.

References

Altschul, S.F., Gish, W., Miller, W., Myers, E.W., and Lipman, D.J. (1990). Basic local alignment search tool. J. Mol. Biol. *215*, 403–410.

Beckmann, G., Hanke, J., Bork, P., and Reich, J.G. (1998). Merging extracellular domains: fold prediction for laminin G-like and amino-terminal thrombospondin-like modules based on homology to pentraxins. J. Mol. Biol. *275*, 725–730.

Bork, P., Hofmann, K., Bucher, P., Neuwald, A.F., Altschul, S.F., and Koonin, E.V. (1997). A superfamily of conserved domains in DNA damage-responsive cell cycle checkpoint proteins. FASEB J. *11*, 68–76.

Carney, J.P., Maser, R.S., Olivares, H., Davis, E.M., Le Beau, M., Yates, J.R., III, Hays, L., Morgan, W.F., and Petrini, J.H.J. (1998). The hMre11/hRad50 protein complex and Nijmegen breakage syndrome: linkage of double-strand break repair to the cellular DNA damage response. Cell *93*, this issue, 477–486.

Chrzanowska, K.H., Kleijer, W.J., Krajewska Walasek, M., Bialecka, M., Gutkowska, A., Goryluk Kozakiewicz, B., Michalkiewicz, J., Stachowski, J., Gregorek, H., Lyson Wojciechowska, G., et al. (1995). Eleven Polish patients with microcephaly, immunodeficiency, and chromosomal instability: the Nijmegen breakage syndrome. Am. J. Med. Genet. *57*, 462–471.

Concannon, P., and Gatti, R.A. (1997). Diversity of *ATM* gene mutations detected in patients with ataxia-telangiectasia. Hum. Mutat. *10*, 100–107.

Digweed, M. (1993). Human genetic instability syndromes: single gene defects with increased risk of cancer. Toxicol. Lett. *67*, 259–281.

Dolganov, G.M., Maser, R.S., Novikov, A., Tosto, L., Chong, S., Bressan, D.A., and Petrini, J.H. (1996). Human Rad50 is physically associated with human Mre11: identification of a conserved multiprotein complex implicated in recombinational DNA repair. Mol. Cell. Biol. *16*, 4832–4841.

Gabriel, S.E., Brigman, K.N., Koller, B.H., Boucher, R.C., and Stutts, M.J. (1994). Cystic fibrosis heterozygote resistance to cholera toxin in the cystic fibrosis mouse model. Science *266*, 107–109.

Hanawalt, P., and Painter, R. (1985). On the nature of a DNA-processing defect in ataxia-telangiectasia. In Ataxia-Telangiectasia: Genetics, Neuropathology, and Immunology of a Degenerative Disease of Childhood, R.A. Gatti and M. Swift, eds. (New York: Alan R. Liss Inc.), pp. 67–71.

Hendrickson, E.A. (1997). Cell-cycle regulation of mammalian DNA double-strand-break repair. Am. J. Hum. Genet. *61*, 795–800.

Hofmann, K., and Bucher P. (1995). The FHA domain: a putative nuclear signaling domain found in protein kinases and transcription factors. Trends Biochem. Sci. *20*, 347–349.

Hudson, T.J., Stein, L.D., Gerety, S.S., Ma, J., Castle, A.B., Silva, J., Slonim, D.K., Baptista, R., Kruglyak, L., Xu, S.H., et al. (1995). An STS-based map of the human genome. Science *270*, 1945–1954.

Jaspers, N.G., Gatti, R.A., Baan, C., Linssen, P.C., and Bootsma, D. (1988a). Genetic complementation analysis of ataxia telangiectasia and Nijmegen breakage syndrome: a survey of 50 patients. Cytogenet. Cell Genet. *49*, 259–263.

Jaspers, N.G., Taalman, R.D., and Baan, C. (1988b). Patients with an inherited syndrome characterized by immunodeficiency, microcephaly, and chromosomal instability: genetic relationship to ataxia telangiectasia. Am. J. Hum. Genet. *42*, 66–73.

Jongmans, W., Vuillaume, M., Chrzanowska, K., Smeets, D., Sperling, K., and Hall, J. (1997). Nijmegen breakage syndrome cells fail to induce the p53-mediated DNA damage response following exposure to ionizing radiation. Mol. Cell Biol. *17*, 5016–5022.

Komatsu, K., Matsuura, S., Tauchi, H., Endo, S., Kodama, S., Smeets, D., and Weemaes, C. (1996). The gene for Nijmegen breakage syndrome (*V2*) is not located on chromosome 11. Am. J. Hum. Genet. *58*, 885–888.

Lichter, P., and Cremer, T. (1992). Chromosome analysis by nonisotopic in situ hybridization. In Human Cytogenetics: A Practical Approach, Second Edition, D.E. Rooney and B.H. Czepulkowski, eds. (Oxford: IRL Press at Oxford University Press), pp 157–192.

Matsuura, K., Balmukhanov, T., Tauchi, H., Weemaes, C., Smeets, D., Chrzanowska, K., Endou, S., Matsuura, S., and Komatsu, K. (1998). Radiation induction of p53 in cells from Nijmegen breakage syndrome is defective but not similar to ataxia-telangiectasia. Biochem. Biophys. Res. Commun. *242*, 602–607.

Meyn, M.S. (1995). Ataxia-telangiectasia and cellular responses to DNA damage. Cancer Res. *55*, 5991–6001.

Morral, N., Bertranpetit, J., Estivill, X., Nunes, V., Casals, T., Gimenez, J., Reis, A., Varon-Mateeva, R., Macek, M., Jr., Kalaydjieva, L., et al. (1994). The origin of the major cystic fibrosis mutation (delta F508) in European populations. Nat. Genet. *7*, 169–175.

Orita, M., Suzuki, Y., Sekiya, T., and Hayashi, K. (1989). Rapid and sensitive detection of point mutations and DNA polymorphisms using the polymerase chain reaction. Genomics *5*, 874–879.

Pearson, W.R., and Lipman, D.J. (1988). Improved tools for biological sequence comparison. Proc. Natl. Acad. Sci. USA *85*, 2444–2448.

Petrini, J.H., Walsh, M.E., DiMare, C., Chen, X.N., Korenberg, J.R., and Weaver, D.T. (1995). Isolation and characterization of the human MRE11 homologue. Genomics *29*, 80–86.

Platzer, M., Rotman, G., Bauer, D., Uziel, T., Savitsky, K., Bar-Shira, A., Gilad, S., Shiloh, Y., and Rosenthal, A. (1997) Ataxia-telangiectasia locus: sequence analysis of 184 kb of human genomic DNA containing the entire *ATM* gene. Genome Res. *7*, 592–605.

Saar, K., Chrzanowska, K.H., Stumm, M., Jung, M., Nurnberg, G., Wienker, T.F., Seemanova, E., Wegner, R.D., Reis, A., and Sperling, K. (1997). The gene for the ataxia-telangiectasia variant, Nijmegen breakage syndrome, maps to a 1-cM interval on chromosome 8q21. Am. J. Hum. Genet. *60*, 605–610.

Savitsky, K., Bar Shira, A., Gilad, S., Rotman, G., Ziv, Y., Vanagaite, L., Tagle, D.A., Smith, S., Uziel, T., Sfez, S., et al. (1995). A single ataxia telangiectasia gene with a product similar to PI-3 kinase. Science *268*, 1749–1753.

Savov, A., Angelicheva, D., Jordanova, A., Eigel, A., and Kalaydjieva, L. (1992). High percentage acrylamide gels improve resolution in SSCP analysis. Nucleic Acids Res. *20*, 6741–6742.

Schuler, G.D., Altschul, S.F., and Lipman., D.J. (1991). A workbench for multiple alignment construction and analysis. Proteins *9*, 180–190.

Schuler, G.D., Boguski, M.S., Stewart, E.A., Stein, L.D., Gyapay, G., Rice, K., White, R.E., Rodriguez-Tome, P., Aggarwal, A., Bajorek, E., et al. (1996). A gene map of the human genome. Science *274*, 540–546.

Seyschab, H., Schindler, D., Friedl, R., Barbi, G., Boltshauser, E., Fryns, J.P., Hanefeld, F., Korinthenberg, R., Krageloh Mann, I., Scheres, J.M., et al. (1992). Simultaneous measurement, using flow cytometry, of radiosensitivity and defective mitogen response in ataxia telangiectasia and related syndromes. Eur. J. Pediatr. *151*, 756–760.

Shiloh, Y. (1997). Ataxia-telangiectasia and the Nijmegen breakage syndrome: related disorders but genes apart. Annu. Rev. Genet. *31*, 635–662.

Stumm, M., Sperling, K., and Wegner, R.D. (1997). Noncomplementation of radiation-induced chromosome aberrations in ataxia-telangiectasia/ataxia-telangiectasia-variant heterodikaryons. Am. J. Hum. Genet. *60*, 1246–1251.

Taalman, R.D., Jaspers, N.G., Scheres, J.M., de Wit, J., and Hustinx, T.W. (1983). Hypersensitivity to ionizing radiation, in vitro, in a new chromosomal breakage disorder, the Nijmegen breakage syndrome. Mutat. Res. *112*, 23–32.

Troelstra, C., and Jaspers, N.G. (1994). Recombination and repair. Ku starts at the end. Curr. Biol. *4*, 1149–1151.

van der Burgt, I., Chrzanowska, K.H., Smeets, D., and Weemaes, C. (1996). Nijmegen breakage syndrome. J. Med. Genet. *33*, 153–156.

Wang, J., Dong, X., Myung, K., Hendrickson, E.A., and Reeves, W.H. (1998). Identification of two domains of the p70 Ku protein mediating dimerization with p80 and DNA binding. J. Biol. Chem. *273*, 842–848.

Weemaes, C.M., Hustinx, T.W., Scheres, J.M., van Munster, P.J., Bakkeren, J.A., and Taalman, R.D. (1981). A new chromosomal instability disorder: the Nijmegen breakage syndrome. Acta Paediatr. *70*, 557–564.

Wegner, R.D., Metzger, M., Hanefeld, F., Jaspers, N.G., Baan, C., Magdorf, K., Kunze, J., and Sperling, K. (1988). A new chromosomal instability disorder confirmed by complementation studies. Clin. Genet. *33*, 20–32.

Wegner, R.D., Chrzanowska, K.H., Sperling, K., and Stumm, M. (1998). Ataxia-telangiectasia variants. In Primary Immunodeficiency Diseases, a Molecular and Genetic Approach, H.D. Ochs, E. Smith, and G. Puck, eds. (Oxford: Oxford University Press), in press.

GenBank Accession Numbers

The accession numbers for the sequence reported in this paper are AF0513334 and AF049895.